SCIENCE AND TECHNOLOGY OF ADVANCED MATERIALS
2019, VOL. 20, NO. 1, 758–773
https://doi.org/10.1080/14686996.2019.1631716

Taylor & Francis
Taylor & Francis Group

FOCUS ISSUE REVIEW

OPEN ACCESS Check for updates

Modulation of surface physics and chemistry in triboelectric energy harvesting technologies

Bo-Yeon Lee[a,b], Dong Hyun Kim[a], Jiseul Park[c], Kwi-Il Park[d], Keon Jae Lee[a] and Chang Kyu Jeong[c,e]

[a]Department of Materials Science and Engineering, Korea Advanced Institute of Science and Technology (KAIST), Daejeon, Republic of Korea;
[b]Department of Nature-Inspired Nano-convergence System, Korea Institute of Machinery and Materials (KIMM), Daejeon, Republic of Korea;
[c]Division of Advanced Materials Engineering, Chonbuk National University, Jeonju, Republic of Korea;
[d]School of Materials Science and Engineering, Kyungpook National University, Daegu, Republic of Korea;
[e]Hydrogen and Fuel Cell Research Center, Chonbuk National University, Jeonju, Republic of Korea

ABSTRACT

Mechanical energy harvesting technology converting mechanical energy wasted in our surroundings to electrical energy has been regarded as one of the critical technologies for self-powered sensor network and Internet of Things (IoT). Although triboelectric energy harvesters based on contact electrification have attracted considerable attention due to their various advantages compared to other technologies, a further improvement of the output performance is still required for practical applications in next-generation IoT devices. In recent years, numerous studies have been carried out to enhance the output power of triboelectric energy harvesters. The previous research approaches for enhancing the triboelectric charges can be classified into three categories: i) materials type, ii) device structure, and iii) surface modification. In this review article, we focus on various mechanisms and methods through the surface modification beyond the limitations of structural parameters and materials, such as surficial texturing/patterning, functionalization, dielectric engineering, surface charge doping and 2D material processing. This perspective study is a cornerstone for establishing next-generation energy applications consisting of triboelectric energy harvesters from portable devices to power industries.

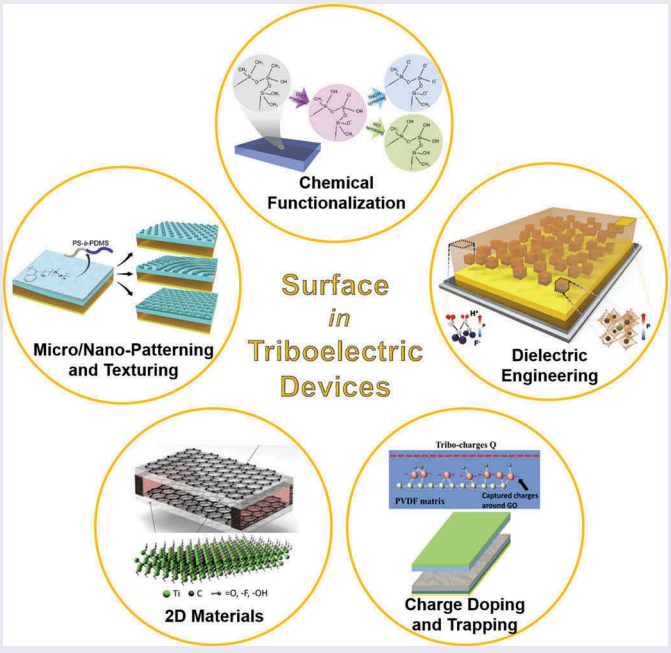

ARTICLE HISTORY
Received 30 March 2019
Revised 11 June 2019
Accepted 11 June 2019

KEYWORDS
Energy harvesting; triboelectric; tribo-electrification; surface engineering; nanogenerator

CLASSIFICATION
50 Energy materials; 202 Dielectrics / Piezoelectrics / Insulators; 206 Energy conversion / transport / storage / recovery; 212 Surface and interfaces

1. Introduction

With the advent of the Fourth Industrial Revolution and the Internet of Things (IoTs), the demand of diverse sensors that can interactively communicate with users has increased dramatically [1–4]. Unlike typical ones, these devices should be comfortable to

CONTACT Keon Jae Lee keonlee@kaist.ac.kr Department of Materials Science and Engineering, Korea Advanced Institute of Science and Technology (KAIST), Daejeon, Republic of Korea; Chang Kyu Jeong ckyu@jbnu.ac.kr Division of Advanced Materials Engineering, Chonbuk National University, Jeonju, Republic of Korea

carry or wear or even attach to curved surfaces. However, conventional battery is not suitable for the power supply of next-generation IoT sensing devices due to its several challenges such as the large volume, the inflexibility and the periodic replacement. In this respect, an energy harvesting technology is newly emerging as one solution that can substitute or supplement the existing batteries [5–10]. Especially, a flexible type of mechanical energy harvester converting the kinetic energy into the electricity has attracted much attention because it can provide the sustainable energy in isolated, indoor environment and biomechanical conditions [11–17].

A piezoelectric energy harvester is one of the ways to harvest mechanical energy, which has been widely investigated by many researchers [18–30]. When a piezoelectric device is deformed by an external mechanical stress, a dipole moment is changed inside the piezoelectric material, and thereby an electric charge is generated [31–37]. Although inorganic ceramics such as a lead zirconate titanate (PZT) or organic polymers such as polyvinylidene fluoride (PVDF) were widely used as active materials of energy harvesters, but the brittle nature and the thick thickness or the low piezoelectric coefficient caused limitations in the various applications [38–44]. In recent years, high-performance flexible energy harvesters based on composites or inorganic thin films were successfully developed with the advanced fabrication processes, which are suitable for diverse self-powered biomonitoring and biomedical sensors [45–52]. Nevertheless, energy harvesters still have some disadvantages such as restricted performance and materials limitation to be commercialized.

To extend energy harvesting technology beyond the piezoelectric energy harvester, a new type of an energy harvesting device was suggested in 2012, called triboelectric generator (TEG) or energy harvester [15]. The basic structure of the TEG based on the coupling effect of the contact electrification and the electrostatic induction is composed of two contact (friction) films with proper electrode positioning [7,53]. Note that the triboelectric effect is a well-known phenomenon that two surfaces having different triboelectric property become electrically charged during mechanical contacts [54–57]. The surface potential difference is generated by the tribocharges resulting from the contact between the surfaces having different charge affinity, thereby inducing electron flow from one to the other electrodes throughout an external circuit to keep the electrostatic equilibrium [58–61]. Based on the working principle, the output performance of TEGs is basically determined by tribocharges [62]. Therefore, considerable efforts have been thus made to increase the amount of tribocharges on the surface. Previous research approaches can be largely divided into three categories such as material pair selection [63–67], device structural design [68–73], and surface modification [74–84]. First, from the viewpoint of material pair election, all materials have the different triboelectric polarity, which means that they have the relative tendency to accept or donate surface charges during contacts [55,66]. The amount of transferred charges becomes higher with the larger difference in the triboelectric polarity for contact surfaces, and vice versa. Accordingly, two contact materials of TEGs are generally chosen far apart each other in the triboelectric series where materials are listed in the order of relative triboelectric polarity [64,67]. Furthermore, materials not listed in the typical triboelectric series can be also evaluated and considered by utilizing surface analysis equipment [66,85,86]. Another way to improve the performance is the optimization of the device structure, such as sliding-mode, rotating-type, non-contact mode, and so forth [68–73]. The other approach is physical and chemical modifications of contact surfaces. This method is an effective way to further maximize the output performance of the optimized device with material selection and structural optimization. The physical modification refers to the increase of contact surface area through the introduction of micro-/nano-structures [66,75,77–80]. This contributes to the increase of the total transferred charges. In addition, the control of surface potential through the chemical modification can make the large difference in the triboelectric polarity between contact surfaces [80–84]. Therefore, there have been diverse researches to modulate the surface potential of contact materials.

Herein, we review the important approaches and methods to modulate materials surface physically and chemically for enhancing triboelectric energy harvesting performance. The principle of triboelectric energy harvesting is first described in a representative device structure. As aforementioned, the crucial mechanism of the triboelectric energy harvesters is based on the frictional electrification by mechanical contacts or slides between two different materials, such as polymers, metals, ceramics, and even liquids [87]. To achieve record-high energy harvesting performance in the triboelectric devices, the electrified surface charges after the mechanical input should be enhanced using various physical or chemical approaches. In the early stages of triboelectric device research, the random surface morphologies were applied to the devices using intrinsic roughness or plasma etching, to name a few [3,88,89]. However, they presented serious demerits such as morphological limitation, poor controllability, unavailable materials, and so on. As shown in Figure 1, we introduce the recently reported advances in surface engineering of triboelectric energy harvesting technologies, such

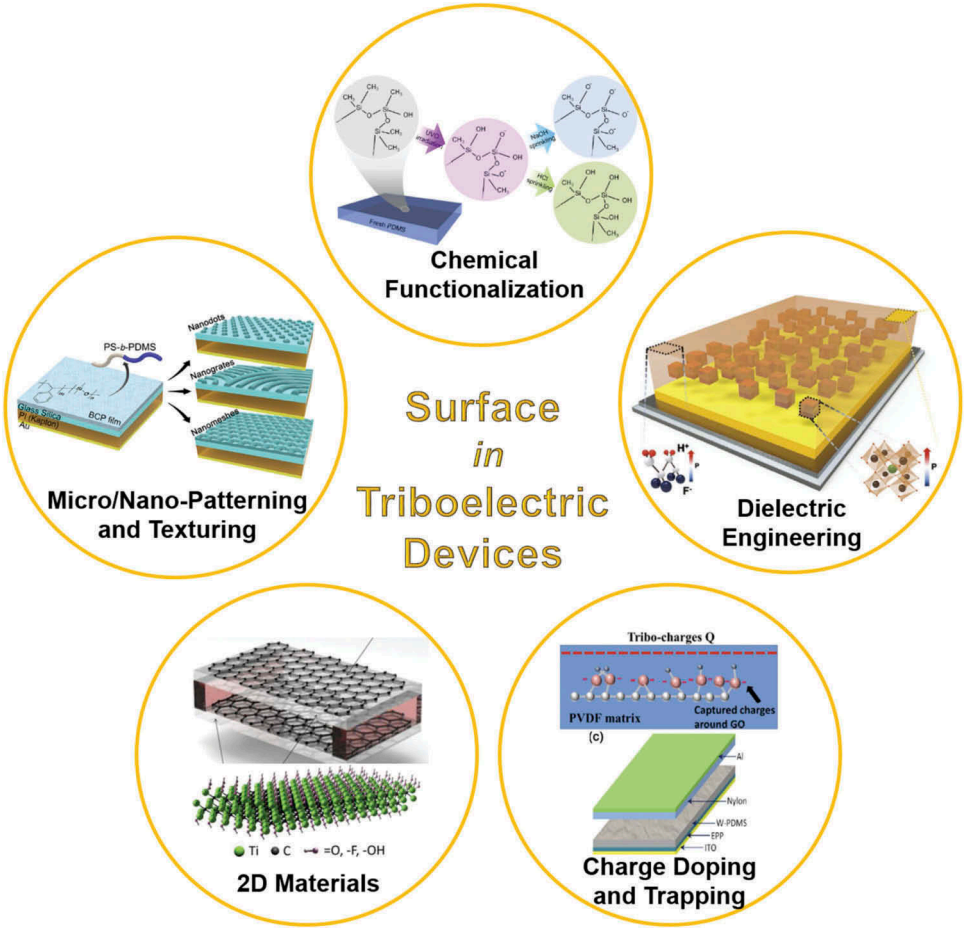

Figure 1. Outline of surface engineering for enhancing performance of triboelectric energy harvesting devices. Reprinted with permission from [77,100,108,110,120,123,124].

as surface texturing/patterning, chemical functionalization, dielectric engineering, charge doping, and two-dimensional (2D) materials processing.

2. Principle of triboelectric energy harvesting

Figure 2(a) shows a representative example of the triboelectric energy harvester for the metal-to-insulator in a contact-separation mode device [90]. Based on the triboelectric series, electrons (or anions) are injected from the silver (Ag) electrode to the polytetrafluoroethylene (PTFE) surface, inducing the net negative charges (Q) on the PTFE part. A schematic equivalent circuit of the triboelectric device with the external load (R) is depicted in Figure 2(b-d). Note that the device can be considered as a flat-plate capacitor with a distance-changeable air gap. The charge density of the PTFE surface is σ, that of copper (Cu) electrode is σ_1, and that of Ag upper surface is σ_2 (Figure 2(b)). Assuming the uniformly distributed charges and the equilibrium state, then we can derive

$$\sigma_1 = -\sigma - \sigma_2 \tag{1}$$

$$\sigma_1 = -\frac{\sigma}{1 + \frac{d_1}{d_2 \varepsilon_{rp}}} \tag{2}$$

where d_1 and ε_{rp} are the thickness and the permittivity of PTFE, respectively. We postulate that the charge Q is relatively stable for a long duration time. Therefore, σ_1 is affected by the distance of air gap (d_2). The charges between Cu and Ag electrodes should be redistributed by the change of d_2, resulting in the voltage potential between the gap and the current generation through the circuit load R. When the triboelectric generator is pressed (Figure 2(c)), the gap distance decreases, resulting in the reduction of σ_1 according to the Equation 2. Thus, an instantaneous positive current is generated. Once the device is mechanically released again (Figure 2(d)), the air gap reverts back to the original distance. Hence, the surface charge σ_1 increases, corresponding to the restoration of the air gap distance d_2, which produces an instantaneous negative current signal. The current signals are shown in Figure 2(e), and they can be merged when multiple devices are connected in parallel according to their polarity (Figure 2(f)). It should be mentioned that the basic working mechanisms of all triboelectric devices are similar although there are other materials types (i.e., insulator-to-insulator type) and/or diverse device structures (e.g., sliding, rotating, and single electrode modes).

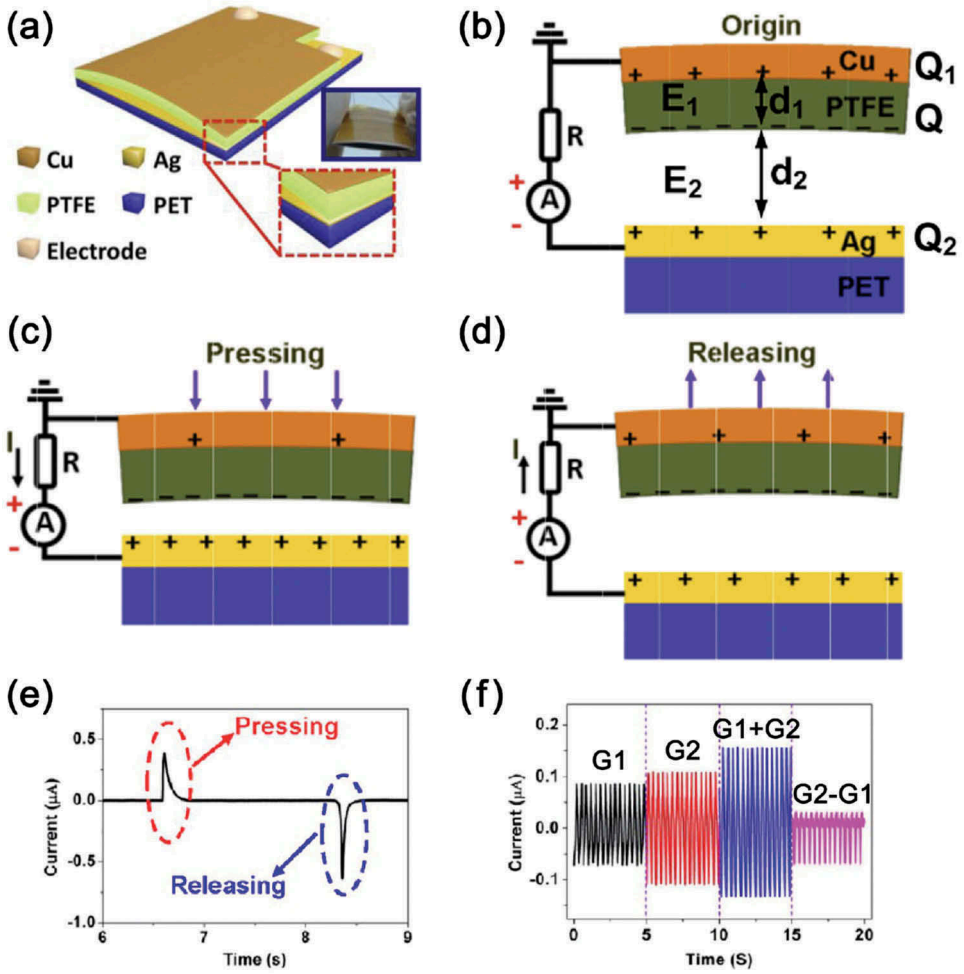

Figure 2. (a) Schematic illustration and photograph of a simple-structured triboelectric energy harvester of the metal-to-insulator type in contact-separation mode. Equivalent circuits of the triboelectric energy harvesting system with an external load when the device is in (b) original, (c) pressed, and (d) released states, and (e) corresponding generated current signals during the single cycle. (f) Linear superposition tests of two triboelectric generators (G1 and G2) connected each other in parallel with same and opposite polarity. Reprinted with permission from [90]. Copyright 2013 Elsevier.

3. Surface texturing and patterning

Figure 3 shows the examples of methods to improve the output performance of triboelectric energy harvesters through the introduction of a micro-/nano-structures on the surface contact layers. These structures mainly contribute to enlargement of effective contact area, resulting in the enhancement of the output performance. For example, the hierarchical microstructure fabricated by ultrafast laser, as shown in Figure 3(a), resulted in the contact-area increment between friction layers, thereby increasing the output performance of the triboelectric energy harvesters [91]. Compared to the triboelectric energy harvester based on pristine polydimethylsiloxane (PDMS), the triboelectric energy harvester based on micro-structured PDMS exhibited at least two times larger output power density. Moreover, laser processing has various advantages such as direct pattering, high speed and facile adjustability [92]. Lee et al. also presented that the surface morphology can be easily modified by the presence of metallic nanowires beneath the friction layer, as shown in Figure 3(b) [66]. Consequently, the surface roughness increased more than three times, and the enlarged surface area contributed in part to the improved output power of triboelectric devices. Similarly, Figure 3(c) describes that the nanoparticle-based surface modification also plays an important role in the enhancement of the output power of triboelectric energy harvesters [75]. Physically, the bumpy surface by the synthesized and self-assembled gold (Au) nanoparticles provides a larger contact area than the flat gold thin film does.

Some researchers have applied highly advanced nanotechnology to the surface patterning for triboelectric energy harvesting devices. Jeong et al. demonstrated the robust and noteworthy way to triboelectric generators with nanoscale tunable surface using very controllable nanostructures via block copolymer (BCP) self-assembly processes [77]. The BCP nanopatterning and nanolithography is a very powerful approach for bottom-up nanofabrication processes to achieve various device applications [93,94]. As shown in Figure 4(a), various silica surface nanopatterns including nanodots,

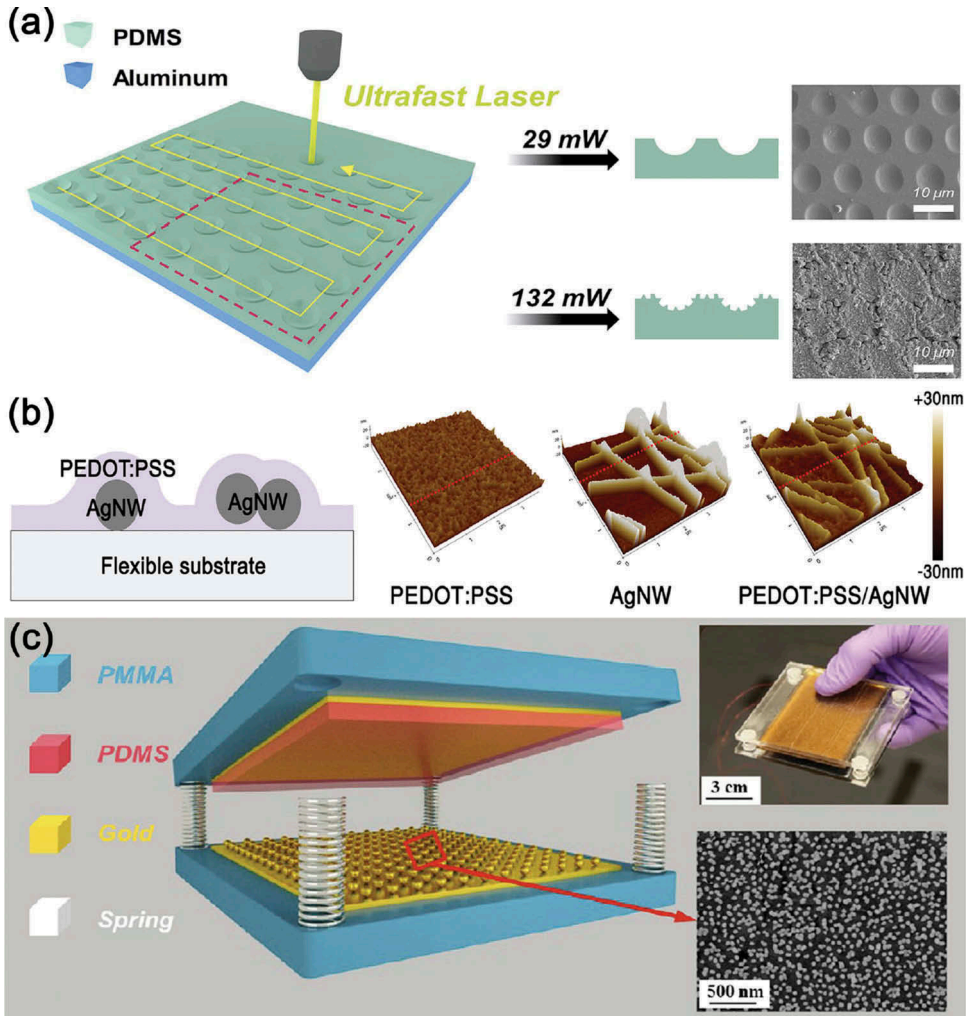

Figure 3. (a) Schematics of the fabrication of laser-irradiated (LI) PDMS using ultrafast laser, and corresponding scanning electron microscopy (SEM) images of the LI-PDMS at laser power of 29 mW and 132 mW. Reprinted with permission from [91]. Copyright 2017 Elsevier. (b) Schematics of the enlarged cross-sectional view of PEDOT:PSS/AgNW layer on a substrate (left). 3D topographic images of PEDOT:PSS, AgNW, and PEDOT:PSS/AgNW films (right). Reprinted with permission from [66]. Copyright 2018 Elsevier. (c) Schematic illustration, photograph, and SEM image of the Au nanoparticles-coated surface based triboelectric generator. Reprinted with permission from [75]. Copyright 2013 American Chemical Society.

nanograte, and nanomeshes on the large-area device were established according to the experimental conditions by the self-assembly of polystyrene-block-polydimethylsiloxane (PS-*b*-PDMS) BCP. In particular, they found the influence of the nanopatterning on the physical frictional events as well as contact surface area in both experimentally and theoretically. Therefore, the corresponding device performance of triboelectric energy harvesters can be also well tuned by the nanoscale surface engineering. This is the one of the representative researches for the surface nanopatterning of triboelectric devices using bottom-up nanotechnologies.

Even though bottom-up nanopatterning technologies have notable nanoscale controllability, they encumber the compatibility to the practical device fabrication because most of commercialized processes are based on top-down processes. To overcome the processing impracticality of most developments in triboelectric energy harvesting devices, the commercialized semiconducting process was adopted to achieve wafer-scale and defect-free nanoscale patterning on both rigid and flexible substrates, as presented in Figure 4(b) [79]. The polycrystalline Si nanograting patterns were fabricated by the conventional optical lithography on an 8-in Si wafer using alternative deposition of spacers and Si layers. Subsequently, the spacer sidewalls were reciprocally formed by spacer deposition and dry etching processes until the polycrystalline Si nanograting patterns were revealed. This modified spacer lithography method is called the multi-spacer pattern downscaling (MS-PaD) method. The uniform nanograting patterns can become much narrower by consuming underneath spacers and Si pattern receivers, which are the core constituents of MS-Pad method. Finally, the large-area sub-50 nm grating nanopattern was well transferred to the flexible plastic film as a replica. The scanning electron microscopy (SEM) image and the iridescent diffraction of optical photograph guarantee the uniform and well-aligned nanopatterned surface (the right panel of Figure 4(b)). The nanograting-based TEG accomplished the

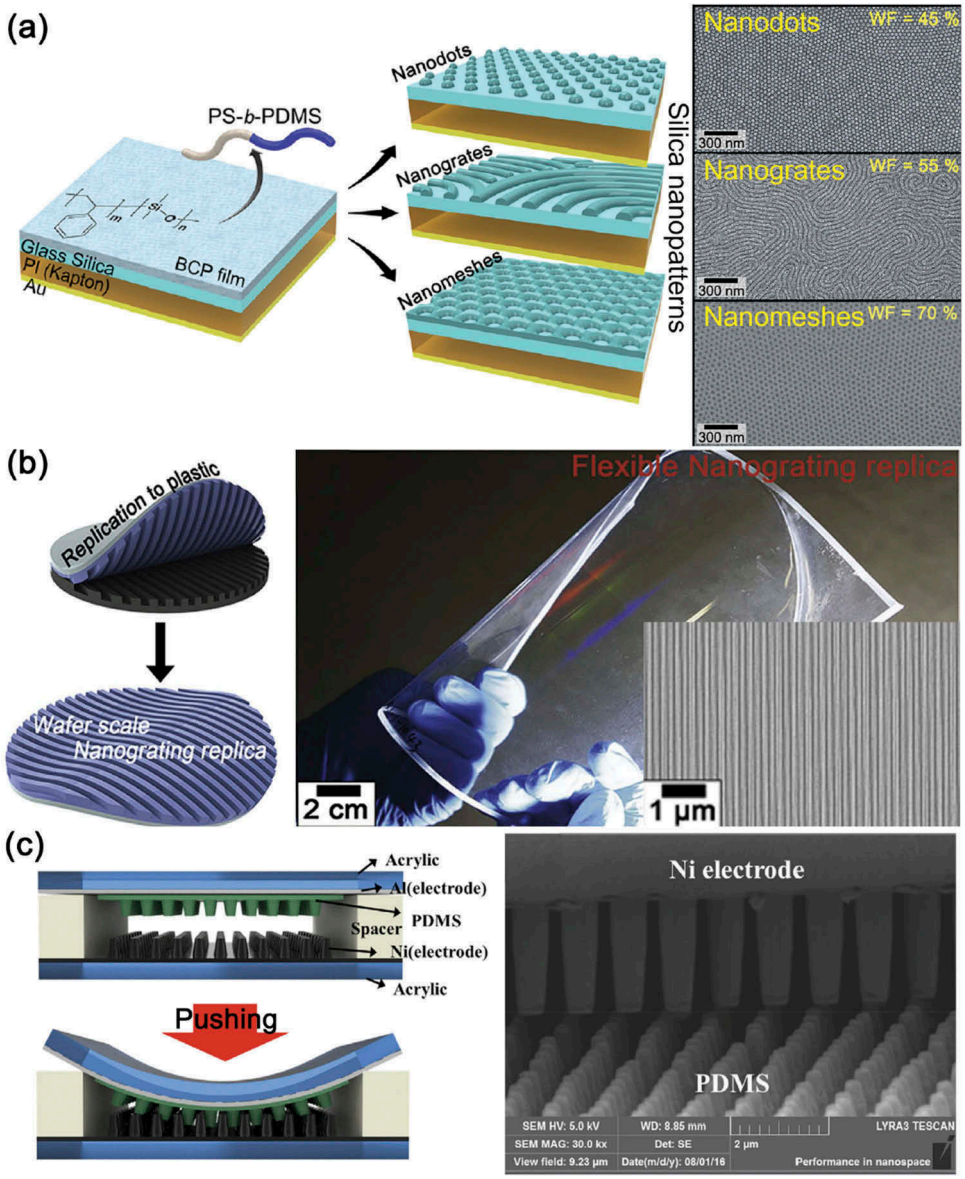

Figure 4. (a) Illustrated fabrication scheme of the nanopatterned surface of the block copolymer (BCP) TEG. The right panels show SEM images of BCP nanopatterned surface established by various self-assembly conditions. Reprinted with permission from [77]. Copyright 2014 American Chemical Society. (b) Schematics of nanograting replication process onto a flexible plastic substrate using ultraviolet (UV)-curable resin. The right panel is the photograph of the wafer-scale and uniform nanograting replica onto the flexible plastic substrate. The inset is the SEM image of the ultra-long and defect-free nanograting pattern of the replica on the flexible substrate. Reprinted with permission from [79]. Copyright 2017 Elsevier. (c) Schematics and SEM image of the interlocked TEG (i-TEG). Reprinted with permission from [95]. Copyright 2016 Elsevier.

performance enhancement of triboelectric energy harvesting, up to 200 times higher power level, compared to the TEG of non-patterned flat surface. Moreover, they systemically demonstrated that the thickness of metal thin film on the nanopatterns can affect the triboelectric energy harvesting performance, firstly indicating the trade-off phenomena in the modulation between electrode conducting and nanopattern flattening effects. Choi et al. fabricated the nature-inspired nanopillar arrays by using the nano-imprint lithography and the electrodeposition [95]. Figure 4(c) presents the structure of nanopillar arrays-based TEG. Through the well-tailored interlocked interfaces, the contact surface area was effectively increased, resulting in the enhanced output voltage and current. Note that the fabrication of surface texturing by micro/nano- patterning and structuring have been utilized as the basis of all surface modulation approaches, which will be introduced as following sections, because the modification of surface morphology and architecture is the basic techniques in the TEGs.

4. Chemical functionalization and modification

The surface potential of the contact materials for triboelectric energy harvesters is well-known to

benefit the improvement of their output performance [96–99]. There have thus been many efforts to control surface chemical properties for the high-output power of triboelectric energy harvesters to increase the difference of triboelectric polarity between two contact surfaces. For example, polar Si-O bonds were substituted for non-polar Si-CH_3 bonds on PDMS surface by using the ultraviolet-ozone (UVO) and the sodium hydroxide treatments, as shown in Figure 5(a). The chemically modified PDMS surface enabled the device to generate large triboelectric charges [100,101], then the modified surface-based TEG showed nearly 15-fold greater current density than the pristine TEG.

Several studies have revealed that fluorinated polymers are one of the most suitable tribo-negative contact materials for triboelectric energy harvesters due to the high electronegativity of fluorine element. Some group obtained the fluoropolymer-coated gecko feet setae-like polypropylene nanowires through a simple and modified physical vapor deposition method [80]. The surface composition with functional groups showing excellent triboelectric property improved the generation efficiency of triboelectric charges, resulting in high output performance, as shown in Figure 5(b). Figure 5(c) shows the triboelectric characteristics of nitro groups and methyl groups attached to cellulose nanofibrils (CNFs) by chemical reaction methods [102]. Cellulose shows almost relatively neutral polarity by its chemical formula, whereas the nitro group and the methyl group have an excellent electron-accepting and electron-donating properties, respectively. The TEGs composed of nitro-CNF and methyl-CNF exhibited the enhanced output power, compared with the pristine CNF-based TEGs. Furthermore, the chemical functionalization of surface contact materials can be used as a practical solution to the friction and wear due to the structural problem of sliding-mode TEGs. As shown in Figure 5(d), the positively charged nylon film partially changed to negatively charged surface through the reactive ion etching (RIE) with a metal mask [103]. The surface-modified sliding-mode TEGs exhibited high stability and strong durability owing to the chemical functionalization.

To more systematically study the effect of surface functional groups on the output performance of triboelectric energy harvesters, various attempts have been made using self-assembled monolayer (SAM) techniques. The kinds of the head group of SAMs effectively alter the surface potential of contact materials. Note that the surface potentials can be analyzed by using scanning Kelvin probe microscopy. As shown in Figure 6(a), four functional groups such as hydroxyl (-OH), ester (-$COOCH_3$), amine (-NH_2) and chloro (-Cl) were formed on the gold (Au) surface through thiol-based SAM functionalization [82]. Among them, the amine groups highly increased the surface chemical potential and thus largely promoted the charge-donating tendency. The output power of the corresponding TEG was enhanced by almost 4 times. A wide spectrum of controllable triboelectric polarity

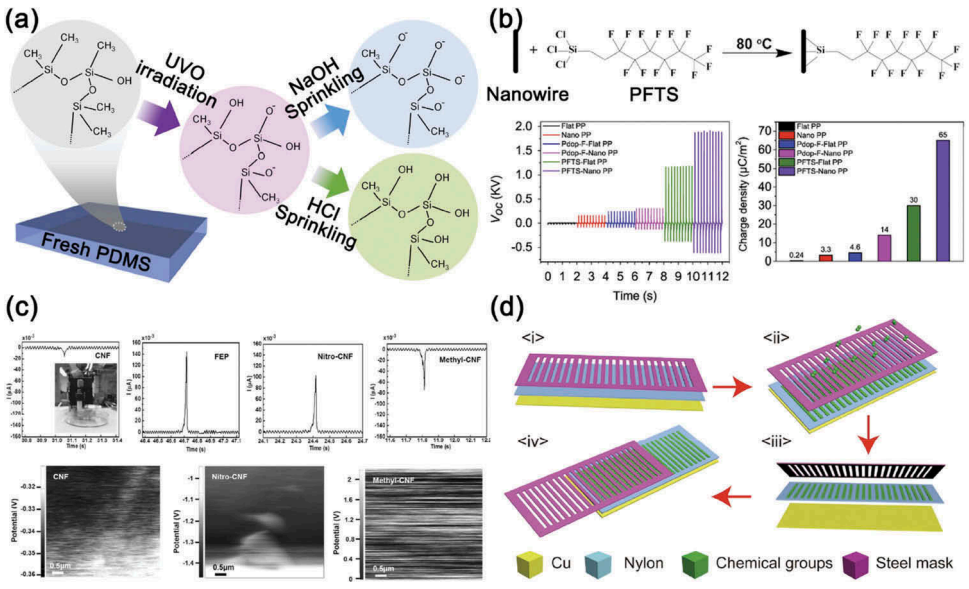

Figure 5. (a) The suggested mechanism of chemical elements and bonds of fresh, UV/O_3, NaOH-, and HCl-treated PDMS surface. Reprinted with permission from [100]. Copyright 2015 Elsevier. (b) Schematics of the surface functionalization with fluorinated organic materials on the PP nanowires. Bottom panels show the voltage generation and the charge density of PP-based TEGs before and after the diverse fluorinated modifications. Reprinted with permission from [80]. Copyright 2016 Elsevier. (c) Current flow obtained from the triboelectric film of CNF, FEP, nitro-CNF, and methyl-CNF during a contact-separation cycle with Ga-In eutectic liquid (top). The scanning Kelvin probe microscopy (SKPM) surface potential mapping of pristine CNF, nitro-CNF, and methyl-CNF (bottom). Reprinted with permission from [102]. Copyright 2017 John Wiley & Sons. (d) Schematics of the reactive ion etching (RIE) and the device fabrication processes of the S-TEG-CGG. Reprinted with permission from [103]. Copyright 2017 American Chemical Society.

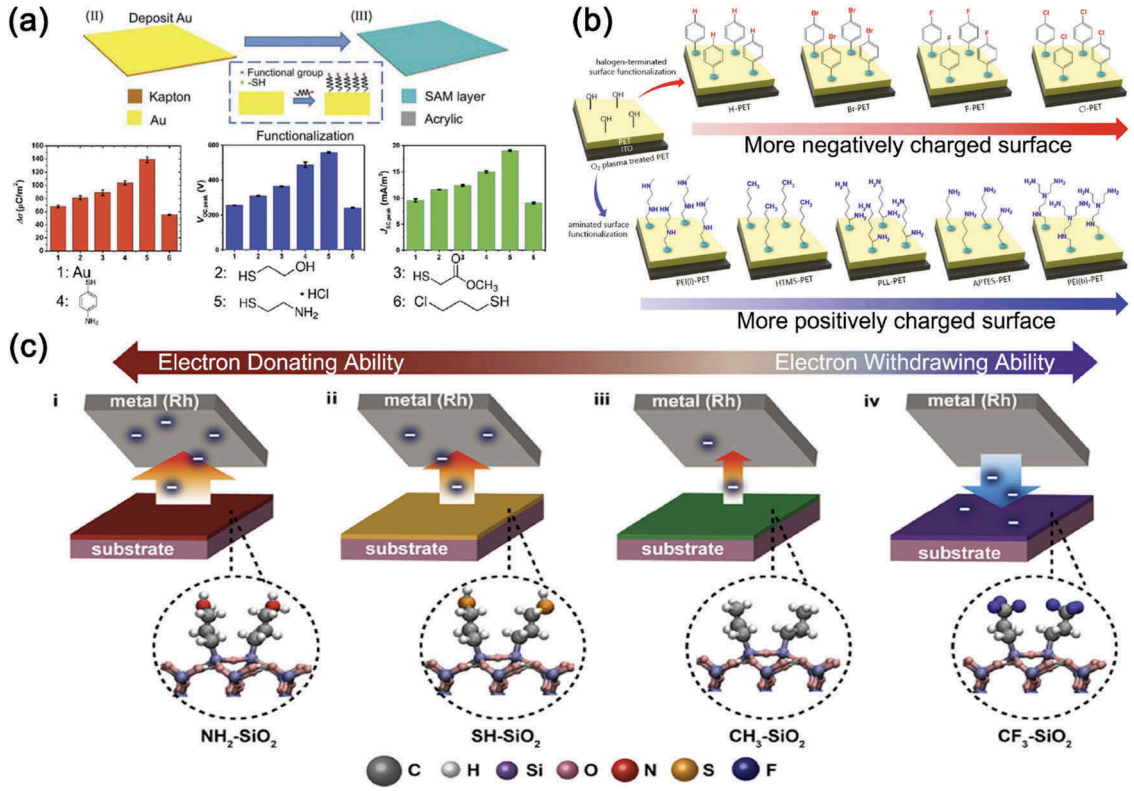

Figure 6. (a) A step in the fabrication process of TEG devices for the thiol-SAM modified Au films. Bottom panels present the comparisons in the transferred charge density, generated voltage, and generated current density of each SAM functionalized TEGs. Reprinted with permission from [82]. Copyright 2016 Royal Society of Chemistry. (b) Schematic illustrations of surface-functionalized polyethylene terephthalate (PET) substrates with various organic molecule head groups for negatively or positively charging. Reprinted with permission from [104]. Copyright 2017 American Chemical Society. (c) Schematic diagram showing the propensity of the triboelectrification from electron-donating to electron-withdrawing layers according to the type of surface dipoles. Reprinted with permission from [86]. Copyright 2016 American Chemical Society.

was obtained through the functionalization of surfaces with the halogen (Br, F and Cl)-containing molecules or the aminated molecules, as shown in Figure 6(b) [104]. Here, hydroxyl surface groups formed by oxygen plasma treatment played a crucial role as strong covalent bonds between the substrate and the molecules. Especially, Cl-terminated surface and branched polyethylenimine (PEI(*b*)) exhibited the most negatively and positively triboelectric properties, respectively. As a result, the Cl:PEI(*b*) contact pair-based TEG generated the large values of maximum output voltage and current density. Byun et al. even demonstrated the modified triboelectric series consisting of SAM-based contact materials. They revealed that the triboelectric property is significantly determined by surface dipoles and electronics states [86]. It was shown that the polarity and amount of triboelectric charges on the surface were well-controlled by modulating the surfaces with a wide range of electron-donating and -accepting functional groups, as shown in Figure 6(c). For instance, the positive surface dipole of CF_3-SiO_2 increased the surface potential, and the negative surface dipole of NH_2, SH, and CH_3 groups decreased the potential. In brief, these SAM-based methods for TEGs are generally simple in operation and effective for widely applicable materials.

Note that the relative polarity and strength of surface potential can be characterized by using Kelvin probe force microscope (KPFM). The measured voltage between a conductive tip of KPFM and a measured surface can reflect the surface potential of triboelectric materials. This surface potential analysis is useful mainly when the materials are not listed in the existing triboelectric series or the surface characteristics have been modified through chemical treatment [66,85,86,105].

5. Charge doping and trapping

In addition to the surface functionalization techniques, the method to add charges on or inside the contact materials can be a great way to enhance the output performance of triboelectric energy harvesters. The large amount of the triboelectric charges distributed on the surface of the contact materials through the charge doping or trapping can lead to a strong driving force for the high-output voltage and current. For example, the surface charge density largely increases through the direct injection of single-polarity charged particles and ions onto the contact surface, as illustrated in Figure 7(a) [81,106]. Through this simple and effective method suggested by Wang et al., a maximum power density of TEGs was improved by as much as 25 times, and the

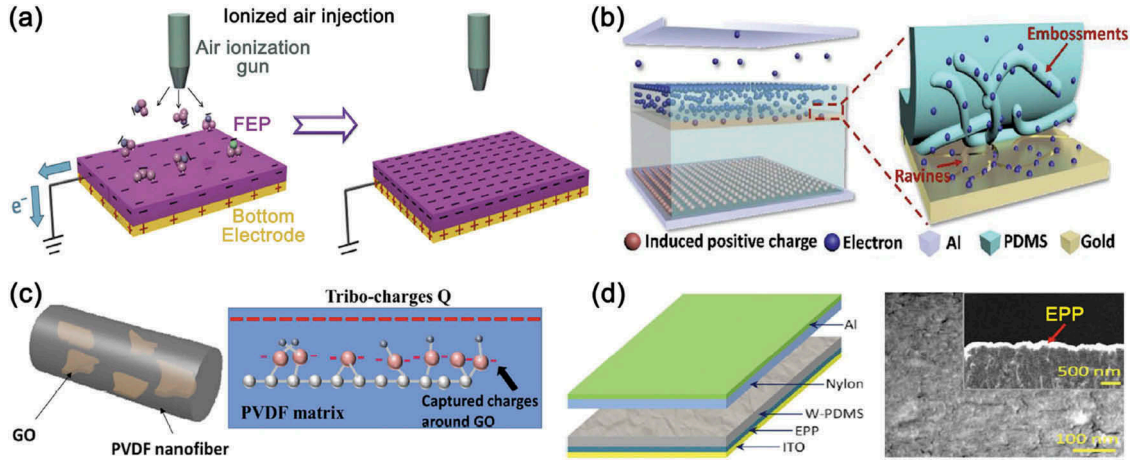

Figure 7. (a) Fabrication illustration of the ionic molecule-injected fluorinated ethylene propylene (FEP) film and the final charge state of the FEP film for the contact-mode TEG. Reprinted with permission from [81]. Copyright 2014 John Wiley & Sons. (b) Schemes of electron drift in the G-TEG device (left) and electron escape from PDMS to Au (right). Reprinted with permission from [107]. Copyright 2018 American Chemical Society. (c) Schemes of PVDF/GO nanofibers presenting the dispersion of GO in the nanofiber (left) and stored charges on the surface of the GO sheet (right). Reprinted with permission from [108]. Copyright 2015 Springer Nature. (d) Device design of the as-fabricated TEG improved by the hole transport layer (left) and the top-view and cross-sectional SEM images of the hole transport layer, showing ethylene glycol (EG)-PEDOT:PSS (EPP) layer coated PDMS surface (right and inset). Reprinted with permission from [110]. Copyright 2016 American Chemical Society.

performance was maintained for several months. Furthermore, they found that the maximum achievable charge density could be more enhanced by the reduction of the thickness in the dielectric film. Trapping charges inside the triboelectric materials also causes the improvement in the output performance of triboelectric energy harvesters. This is because that the loss of triboelectric electrons can be suppressed by trapped sites. The groove structure on an Au layer fabricated by a plasma treatment acted as a trap site of triboelectric charges, as depicted in Figure 7(b) [107]. Similarly, graphene oxide (GO) sheets can be used as trap sites [108,109]. As shown in Figure 7(c), the GO, embedded in the PVDF nanofibers, played a role as charge trapping sites, which improved the output performance of the TEGs [108]. The charges trapped in the GO raised the surface potential of the PVDF nanofibers and even delayed the dissipation of the surface charges. Uddin et al. utilized a polymer mixture, poly(3,4-ethylene dioxythiophene) poly(styrene sulfonate) (PEDOT:PSS), as the charge trapping layer to increase the amount of triboelectric charges [110]. A PEDOT:PSS film, which has been widely used for a hole transport layer, was placed between a contact material and an electrode as, shown in Figure 7(d). This charge accumulator layer accelerated the flow of charges at the interface, thereby contributing to enhanced triboelectric energy harvesting.

6. Dielectric property engineering

Controlling the dielectric property of triboelectric materials can affect the output performance of triboelectric energy harvesters [111–116]. Triboelectric charge density on the contact materials is proportional to the maximum capacitance of the triboelectric energy harvester. It means that the charge density can be increased with the increase of the relative permittivity and the decrease of the thickness of the contact materials.

As shown in Figure 8(a, b), some researchers put the nanoparticles with high permittivity inside the contact materials to increase the dielectric constant of materials [65,117,118]. Chen et al. used the dielectric nanoparticles such as SiO_2, TiO_2, $BaTiO_3$, $SrTiO_3$ filling into PDMS matrices to increase the permittivity of contact materials [65]. Among them, the TEGs using $SrTiO_3$ produced the highest output voltage due to its highest relative permittivity of 300. Accompanying with modulating relative permittivity, they also effectively reduced the thickness of contact materials by forming pores which were fabricated by mixing and removing NaCl salt particles. The output voltage and current density were improved with increasing porosity. They showed the maximum value at the volume ratio of 15% presumably because the relative permittivity also decreases with the increase of the porosity. Chun et al. also developed the high-power TEG based on the Au nanoparticles-embedded porous film [118]. They synthesized a copolymer to increase the dielectric constant of contact materials. As shown in Figure 8(c), PVDF was successfully incorporated with poly(tert-butyl acrylate) (PtBA) through the atom-transfer radical polymerization [119]. The PtBA composed of the functional groups containing π-bonding and polar characteristics enhanced the dipole moment of contact materials, resulting in the improved performance of TEGs. Additionally, the aligned dipoles by poling the contact materials highly spurred the charge-accepting

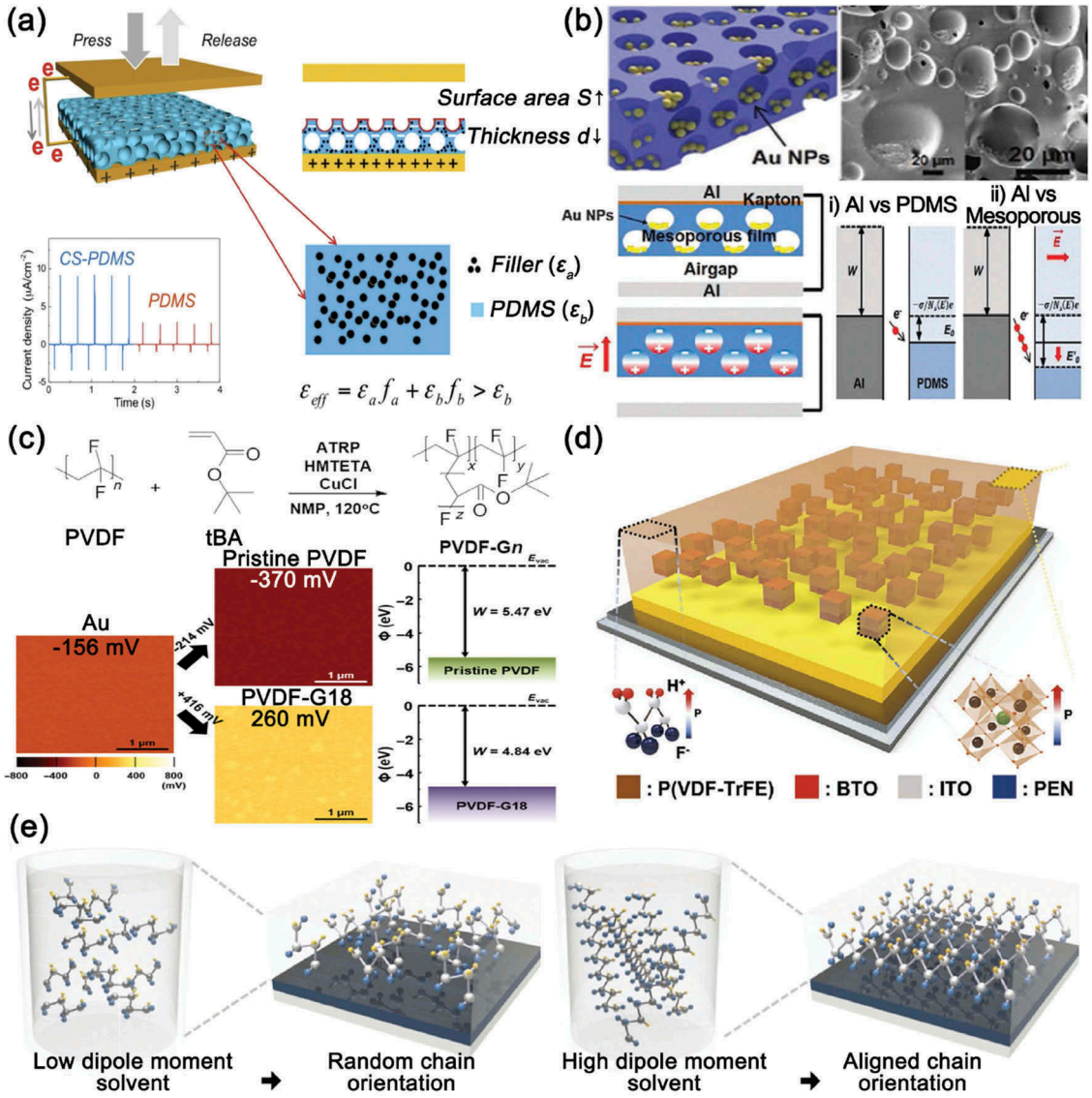

Figure 8. (a) Schematic illustrations of composite sponge PDMS-based TEG (CS-TEG) and its principle of performance enhancement. Reprinted with permission from [65]. Copyright 2016 American Chemical Society. (b) Schematics and SEM image of the mesoporous PDMS film filled with Au nanoparticles (top). Triboelectric charge generation mechanisms of the Au NP-embedded mesoporous triboelectric nanogenerator and schematic energy band diagram (bottom). Reprinted with permission from [118]. Copyright 2015 Royal Society of Chemistry. (c) Simple diagram of synthesis of PVDF-Gn graft copolymer for dielectric-controlled triboelectric energy harvesters (Top). The Kelvin probe force microscopy (KPFM) surface potential distribution images and work function values of pristine PVDF and PVDF-G18 films (bottom). Reprinted with permission from [119]. Copyright 2017 AAAS. (d) Schematic description of the ferroelectric composite for control dielectric properties to enhance triboelectric energy harvesting. Reprinted with permission from [120]. Copyright 2017 John Wiley & Sons. (e) Schematic illustrations of P(VDF-TrFE) solution in low dipole moment solvent and its corresponding film on a substrate (left), and P(VDF-TrFE) solution in high dipole moment solvent and its corresponding film on the substrate (right). Reprinted with permission from [121]. Copyright 2017 John Wiley & Sons.

characteristics of contact materials, thereby further increasing the output power by 20 times. Seung et al. utilized both the effects of the relative permittivity and the polarization on the output power of TEGs. As highlighted in Figure 8(d), the poled ferroelectric P(VDF-TrFE) copolymer mixing with high dielectric $BaTiO_3$ was used as the contact material [120]. As aforementioned, both of electrically manipulated polarization and high dielectric property could induce a very strong surface potential on contact materials. As a result, the TEGs based on this poled P(VDF-TrFE):$BaTiO_3$ showed 150 times higher output power than typical PTFE-based TEGs. In addition to electrical poling method, applying a high dipole moment solvent can be another way to align dipoles in contact materials. The end-to-end chain length and the dipole alignment were enhanced by a high dipole moment solvent such as dimethyl sulfoxide (DMSO), as indicated in Figure 8(e) [121]. Hence, the P(VDF-TrFE) polymer dissolved in the DMSO had a relatively high charge-accepting ability, leading to the output enhancement of triboelectric energy harvesters.

More notably, the shift of effective work function and the corresponding electron transport which had been insisted in the previous reports about ferroelectric (highly dielectric)-induced triboelectric enhancement [111,118] has been denied in reality [57,122]. According to the very recent study, the performance enhancement is almost due to the induction driven by piezoelectric charges [122]. In fact, the correlation between dielectric properties and triboelectric energy harvesting signals is not clearly unveiled, yet. It should be more investigated.

7. Surface with two-dimensional (2D) materials

2D materials are ultrathin nanomaterials which are composed of a few atomic layers, e.g., graphene. Therefore, these specially classified materials can wrap universal interfaces and surfaces with conformal coverage, which can bestow totally different physical and chemical properties upon the original material surface. In other words, adopting 2D materials would result in any strategies mentioned above.

Figure 9(a) displays the energy harvesting performance generated by graphene-based TEGs [123]. Kim et al. demonstrated the flexible transparent graphene-based TEG device using monolayer (1L), bilayer (2L), trilayer (3L), and quadlayer (4L) graphene synthesized on the Cu foils [123]. They provide that the output performance of 2D material-based TEG could depend on the number of graphene layers in terms of the deviation in their work function and friction, which stems from different electronic configurations among different layer stacking features. Dong et al. synthesized an emerging family of 2D layered transition metal carbides and/or nitrides, called MXenes, and applied them to TEG devices, as displayed in Figure 9(b) [124]. MXene materials, which can be modulated by tuning the composition and the functional groups, are conducting matter and exhibit high electronegativity resulting from fluorinated groups. Wu et al. introduced 2D molybdenum disulfide (MoS_2) monolayer sheets inside the triboelectric contact materials, as presented in Figure 9(c) [125]. Similar to the reduced GO sheet, the MoS_2 monolayer has the electron-accepting property [109]. Furthermore, the interface trap states are

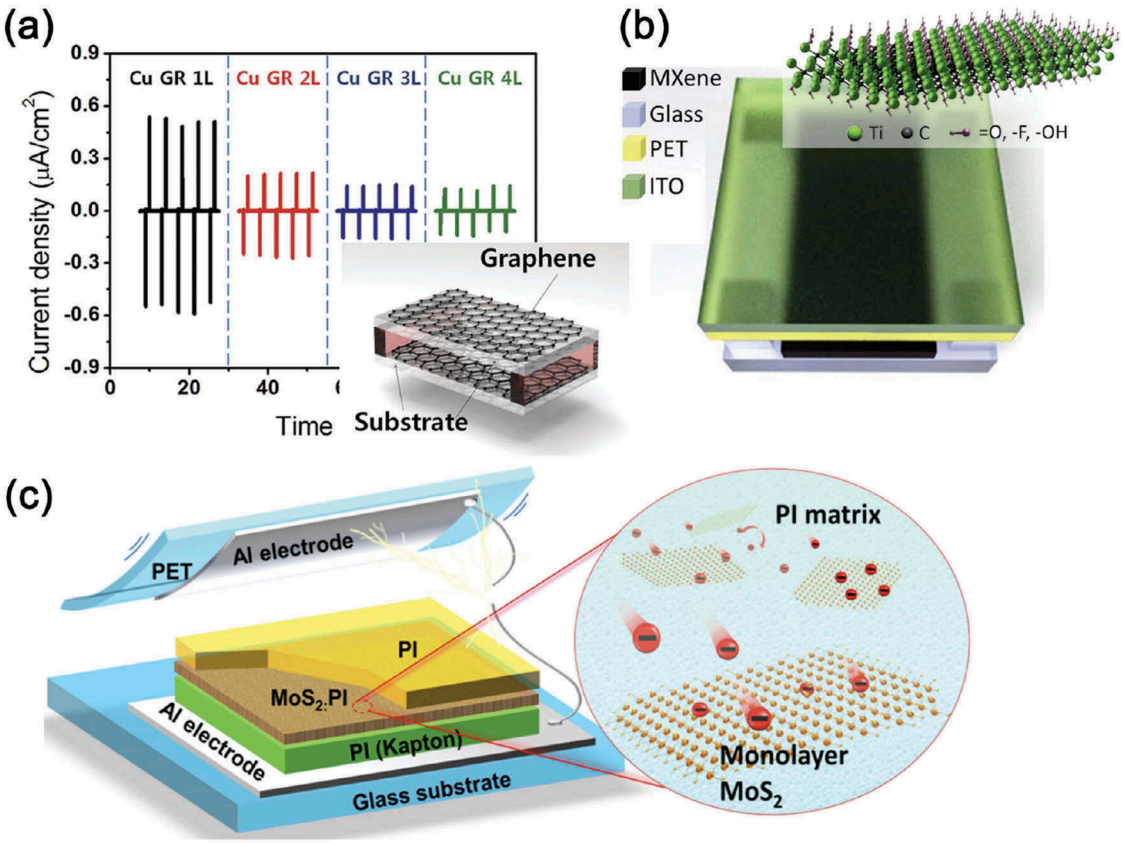

Figure 9. (a) Output current density generated by the Cu foil-grown 1L-, 2L-, 3L-, and 4L-stacked graphene-based TEG under same compressive force. Inset: a schematic illustration of graphene-based transparent TEG device with a spacer structure. Reprinted with permission from [123]. Copyright 2014 John Wiley & Sons. (b) Schematics of MXene TEG (MXene/glass for the bottom electrode) with an air gap between top and bottom electrodes. ITO stands for indium tin oxide and PET for polyethylene terephthalate. Inset: illustration of $Ti_3C_2T_x$ MXene structure. Reprinted with permission from [124]. Copyright 2018 Elsevier. (c) Device structure of the TEG made by the MoS_2 monolayer films (left). Schematics of the electron transfer from the PI matrix to the MoS_2 monolayers (right). Reprinted with permission from [125]. Copyright 2017 American Chemical Society.

distributed in the band gap because of the intrinsically large bandgap energy. Owing to the 2D MoS_2 monolayer, the TEG exhibited 120 times larger power density compared with the pristine TEG. According to these examples, 2D materials have been regarded as new approaches to modulate universal surface for triboelectric device applications [126].

8. Concluding remarks and perspectives

In this review, we have taken account of the representative approaches of physical and chemical surface engineering to enhance triboelectric energy harvesting performance, such as surficial texturing/patterning, chemical functionalization, dielectric engineering, intentional charge doping and 2D material processing, after summarizing the working principle of triboelectric energy harvesting devices. Although the triboelectrification has been a very well-known and fundamental phenomenon to everyone in our life since ancient Greek era, the microscopic mechanisms of tribology in many cases are still ambiguous and dim. Nonetheless, recent developments for triboelectric energy harvesting have demonstrated tremendous advances in power performance through designing device structures and circuit engineering. Due to superficial and incompatible studies between tribology sciences and triboelectric devices, the next-generation research for triboelectric devices is now staggering under the burden of hasty commercialization. To surmount the significant restriction, we need to flash back the scientific basics of tribology and electrification on certain materials surface. Hence, reminding previously reported surface engineering approaches is considerably meaningful. In addition, it is helpful to face the mechanical problem caused by wear and abrasion without vague evasions [127]. This review has highlighted representative studies, not all researches for surface engineering of triboelectric devices. Note that some aforementioned classifications of surface engineering might overlap. Notwithstanding, our review could provide important resources to shed a light on future breakthroughs in this research field by concentrating on surface modulation because most previous review reports have focused on triboelectric device structures, performance and applications. This perspective will turn into the most sought-after outlook in the development of high-performance and practical triboelectric energy harvesting and sensor devices toward commercialization someday. Ultimately, such the development will be expected to provide sustainable power to the next-generation applications from smart IoT sensors to biomedical devices.

Disclosure statement

No potential conflict of interest was reported by the authors.

Funding

This work was supported by the Basic Science Research Program through the National Research Foundation of Korea (NRF) funded by the Ministry of Education [2018R1A6A3A01011608]. This work was supported by the Wearable Platform Materials Technology Center (WMC) [NRF-2016R1A5A1009926]. This work was supported by the National Research Foundation of Korea (NRF) grant funded by the Korea government (MSIT) [NRF-2019R1C1C1002571]. This research was supported by 'Research Base Construction Fund Support Program' funded by Chonbuk National University in 2019.

References

[1] Dagdeviren C, Shi Y, Joe P, et al. Conformal piezoelectric systems for clinical and experimental characterization of soft tissue biomechanics. Nat Mater. 2015;14:728–736.
[2] Wang ZL. Self-powered nanosensors and nanosystems. Adv Mater. 2012;24:280–285.
[3] Fan F-R, Lin L, Zhu G, et al. Transparent triboelectric nanogenerators and self-powered pressure sensors based on micropatterned plastic films. Nano Lett. 2012;12:3109–3114.
[4] Hwang G-T, Annapureddy V, Han JH, et al. Self-powered wireless sensor node enabled by an aerosol-deposited PZT flexible energy harvester. Adv Energy Mater. 2016;6:1600237.
[5] Kuo AD. BIOPHYSICS: harvesting energy by improving the economy of human walking. Science. 2005;309:1686–1687.
[6] Xu S, Qin Y, Xu C, et al. Self-powered nanowire devices. Nat Nanotechnol. 2010;5:366–373.
[7] Wang S, Lin L, Wang ZL. Nanoscale triboelectric-effect-enabled energy conversion for sustainably powering portable electronics. Nano Lett. 2012;12:6339–6346.
[8] Wang ZL, Wu W. Nanotechnology-enabled energy harvesting for self-powered micro-/nanosystems. Angew Chemie Int Ed. 2012;51:11700–11721.
[9] Lee KY, Gupta MK, Kim S-W. Transparent flexible stretchable piezoelectric and triboelectric nanogenerators for powering portable electronics. Nano Energy. 2015;14:139–160.
[10] Lee SH, Jeong CK, Hwang G-T, et al. Self-powered flexible inorganic electronic system. Nano Energy. 2015;14:111–125.
[11] Dagdeviren C, Joe P, Tuzman OL, et al. Recent progress in flexible and stretchable piezoelectric devices for mechanical energy harvesting, sensing and actuation. Extrem Mech Lett. 2016;9:269–281.
[12] Fan FR, Tang W, Wang ZL. Flexible nanogenerators for energy harvesting and self-powered electronics. Adv Mater. 2016;28:4283–4305.
[13] Hwang G-T, Yang J, Yang SH, et al. A reconfigurable rectified flexible energy harvester via solid-state single crystal grown PMN-PZT. Adv Energy Mater. 2015;5:1500051.
[14] Kim DH, Shin HJ, Lee H, et al. In vivo self-powered wireless transmission using biocompatible flexible energy harvesters. Adv Funct Mater. 2017;27:1700341.
[15] Fan F-R, Tian Z-Q, Lin Wang Z. Flexible triboelectric generator. Nano Energy. 2012;1:328–334.

[16] Chen SW, Cao X, Wang N, et al. An ultrathin flexible single-electrode triboelectric-nanogenerator for mechanical energy harvesting and instantaneous force sensing. Adv Energy Mater. 2017;7:1601255.
[17] Jung W-S, Lee M-J, Kang M-G, et al. Powerful curved piezoelectric generator for wearable applications. Nano Energy. 2015;13:174–181.
[18] Dagdeviren C, Yang BD, Su Y, et al. Conformal piezoelectric energy harvesting and storage from motions of the heart, lung, and diaphragm. Proc Natl Acad Sci. 2014;111:1927–1932.
[19] Zhang Z, Yao C, Yu Y, et al. Mesoporous piezoelectric polymer composite films with tunable mechanical modulus for harvesting energy from liquid pressure fluctuation. Adv Funct Mater. 2016;26:6760–6765.
[20] Won SS, Seo H, Kawahara M, et al. Flexible vibrational energy harvesting devices using strain-engineered perovskite piezoelectric thin films. Nano Energy. 2019;55:182–192.
[21] Park JH, Lee HE, Jeong CK, et al. Self-powered flexible electronics beyond thermal limits. Nano Energy. 2019;56:531–546.
[22] Kim S-D, Hwang G-T, Song K, et al. Inverse size-dependence of piezoelectricity in single $BaTiO_3$ nanoparticles. Nano Energy. 2019;58:78–84.
[23] Park K-I, Xu S, Liu Y, et al. Piezoelectric $BaTiO_3$ thin film nanogenerator on plastic substrates. Nano Lett. 2010;10:4939–4943.
[24] Park K-I, Lee M, Liu Y, et al. Flexible nanocomposite generator made of $BaTiO_3$ nanoparticles and graphitic carbons. Adv Mater. 2012;24:2999–3004.
[25] Jeong CK, Kim I, Park K-I, et al. Virus-directed design of a flexible $BaTiO_3$ nanogenerator. ACS Nano. 2013;7:11016–11025.
[26] Park K-I, Jeong CK, Ryu J, et al. Flexible and large-area nanocomposite generators based on lead zirconate titanate particles and carbon nanotubes. Adv Energy Mater. 2013;3:1539–1544.
[27] Jeong CK, Park K-I, Ryu J, et al. Large-area and flexible lead-free nanocomposite generator using alkaline niobate particles and metal nanorod filler. Adv Funct Mater. 2014;24:2620–2629.
[28] Jeong CK, Lee J, Han S, et al. A hyper-stretchable elastic-composite energy harvester. Adv Mater. 2015;27:2866–2875.
[29] Park K-I, Jeong CK, Kim NK, et al. Stretchable piezoelectric nanocomposite generator. Nano Converg. 2016;3:12.
[30] Jeong CK, Han JH, Palneedi H, et al. Comprehensive biocompatibility of nontoxic and high-output flexible energy harvester using lead-free piezoceramic thin film. APL Mater. 2017;5:074102.
[31] Zhang Y, Sun H, Jeong CK. Biomimetic porifera skeletal structure of lead-free piezocomposite energy harvesters. ACS Appl Mater Interfaces. 2018;10:35539–35546.
[32] Zhang Y, Jeong CK, Wang J, et al. Flexible energy harvesting polymer composites based on biofibril-templated 3-dimensional interconnected piezoceramics. Nano Energy. 2018;50:35–42.
[33] Wang X. Piezoelectric nanogenerators—harvesting ambient mechanical energy at the nanometer scale. Nano Energy. 2012;1:13–24.
[34] Seo M-H, Yoo J-Y, Choi S-Y, et al. Versatile transfer of an ultralong and seamless nanowire array crystallized at high temperature for use in high-performance flexible devices. ACS Nano. 2017;11:1520–1529.
[35] Zhang Y, Jeong CK, Yang T, et al. Bioinspired elastic piezoelectric composites for high-performance mechanical energy harvesting. J Mater Chem A. 2018;6:14546–14552.
[36] Chae I, Jeong CK, Ounaies Z, et al. Review on electromechanical coupling properties of biomaterials. ACS Appl Bio Mater. 2018;1:936–953.
[37] Seo J, Kim Y, Park WY, et al. Out-of-plane piezoresponse of monolayer MoS_2 on plastic substrates enabled by highly uniform and layer-controllable CVD. Appl Surf Sci. 2019;487:1356–1361.
[38] Park K-I, Son JH, Hwang G-T, et al. Highly-efficient, flexible piezoelectric PZT thin film nanogenerator on plastic substrates. Adv Mater. 2014;26:2514–2520.
[39] Jeong CK, Cho SB, Han JH, et al. Flexible highly-effective energy harvester via crystallographic and computational control of nanointerfacial morphotropic piezoelectric thin film. Nano Res. 2017;10:437–455.
[40] Khan MB, Kim DH, Han JH, et al. Performance improvement of flexible piezoelectric energy harvester for irregular human motion with energy extraction enhancement circuit. Nano Energy. 2019;58:211–219.
[41] Sun C, Shi J, Bayerl DJ, et al. PVDF microbelts for harvesting energy from respiration. Energy Environ Sci. 2011;4:4508.
[42] Mao Y, Zhao P, McConohy G, et al. Sponge-like piezoelectric polymer films for scalable and integratable nanogenerators and self-powered electronic systems. Adv Energy Mater. 2014;4:1301624.
[43] Jeong CK, Baek C, Kingon AI, et al. Lead-free perovskite nanowire-employed piezopolymer for highly efficient flexible nanocomposite energy harvester. Small. 2018;14:1704022.
[44] Zhang Y, Zhu W, Jeong CK, et al. A microcube-based hybrid piezocomposite as a flexible energy generator. RSC Adv. 2017;7:32502–32507.
[45] Hwang G-T, Park H, Lee J-H, et al. Self-powered cardiac pacemaker enabled by flexible single crystalline PMN-PT piezoelectric energy harvester. Adv Mater. 2014;26:4880–4887.
[46] Hwang G-T, Kim Y, Lee J-H, et al. Self-powered deep brain stimulation via a flexible PIMNT energy harvester. Energy Environ Sci. 2015;8:2677–2684.
[47] Lee HS, Chung J, Hwang G-T, et al. Flexible inorganic piezoelectric acoustic nanosensors for biomimetic artificial hair cells. Adv Funct Mater. 2014;24:6914–6921.
[48] Hwang G-T, Byun M, Jeong CK, et al. Flexible piezoelectric thin-film energy harvesters and nanosensors for biomedical applications. Adv Healthc Mater. 2015;4:646–658.
[49] Park DY, Joe DJ, Kim DH, et al. Self-powered real-time arterial pulse monitoring using ultrathin epidermal piezoelectric sensors. Adv Mater. 2017;29:1702308.
[50] Han JH, Bae KM, Hong SK, et al. Machine learning-based self-powered acoustic sensor for speaker recognition. Nano Energy. 2018;53:658–665.
[51] Han JH, Kwak J-H, Joe DJ, et al. Basilar membrane-inspired self-powered acoustic sensor enabled by highly sensitive multi tunable frequency band. Nano Energy. 2018;53:198–205.
[52] Moorthy B, Baek C, Wang JE, et al. Piezoelectric energy harvesting from a PMN–PT single nanowire. RSC Adv. 2017;7:260–265.
[53] Zhu G, Pan C, Guo W, et al. Triboelectric-generator-driven pulse electrodeposition for micropatterning. Nano Lett. 2012;12:4960–4965.

[54] Mizes HA, Conwell EM, Salamida DP. Direct observation of ion transfer in contact charging between a metal and a polymer. Appl Phys Lett. 1990;56:1597–1599.
[55] Liu C, Bard AJ. Electrons on dielectrics and contact electrification. Chem Phys Lett. 2009;480:145–156.
[56] Lowell J. Surface states and the contact electrification of polymers. J Phys D Appl Phys. 1977;10:65–71.
[57] Baytekin HT, Patashinski AZ, Branicki M, et al. The mosaic of surface charge in contact electrification. Science. 2011;333:308–312.
[58] Xu C, Zi Y, Wang AC, et al. On the electron-transfer mechanism in the contact-electrification effect. Adv Mater. 2018;30:1706790.
[59] Niu S, Liu Y, Wang S, et al. Theoretical investigation and structural optimization of single-electrode triboelectric nanogenerators. Adv Funct Mater. 2014;24:3332–3340.
[60] Niu S, Wang S, Lin L, et al. Theoretical study of contact-mode triboelectric nanogenerators as an effective power source. Energy Environ Sci. 2013;6:3576.
[61] Niu S, Liu Y, Wang S, et al. Theory of sliding-mode triboelectric nanogenerators. Adv Mater. 2013;25:6184–6193.
[62] Dharmasena RDIG, Deane JHB, Silva SRP. Nature of power generation and output optimization criteria for triboelectric nanogenerators. Adv Energy Mater. 2018;8:1802190.
[63] Zhao XJ, Zhu G, Wang ZL. Coplanar induction enabled by asymmetric permittivity of dielectric materials for mechanical energy conversion. ACS Appl Mater Interfaces. 2015;7:6025–6029.
[64] Kim YJ, Lee J, Park S, et al. Effect of the relative permittivity of oxides on the performance of triboelectric nanogenerators. RSC Adv. 2017;7:49368–49373.
[65] Chen J, Guo H, He X, et al. Enhancing performance of triboelectric nanogenerator by filling high dielectric nanoparticles into sponge PDMS film. ACS Appl Mater Interfaces. 2016;8:736–744.
[66] Lee B-Y, Kim S-U, Kang S, et al. Transparent and flexible high power triboelectric nanogenerator with metallic nanowire-embedded tribonegative conducting polymer. Nano Energy. 2018;53:152–159.
[67] Żenkiewicz M, Żuk T, Markiewicz E. Triboelectric series and electrostatic separation of some biopolymers. Polym Test. 2015;42:192–198.
[68] Bai P, Zhu G, Liu Y, et al. Cylindrical rotating triboelectric nanogenerator. ACS Nano. 2013;7:6361–6366.
[69] Zhu G, Chen J, Zhang T, et al. Radial-arrayed rotary electrification for high performance triboelectric generator. Nat Commun. 2014;5:3426.
[70] Lin L, Wang S, Xie Y, et al. Segmentally structured disk triboelectric nanogenerator for harvesting rotational mechanical energy. Nano Lett. 2013;13:2916–2923.
[71] Yang Y, Zhang H, Chen J, et al. Single-electrode-based sliding triboelectric nanogenerator for self-powered displacement vector sensor system. ACS Nano. 2013;7:7342–7351.
[72] Wang S, Lin L, Xie Y, et al. Sliding-triboelectric nanogenerators based on in-plane charge-separation mechanism. Nano Lett. 2013;13:2226–2233.
[73] Zhang H, Yang Y, Su Y, et al. Triboelectric nanogenerator for harvesting vibration energy in full space and as self-powered acceleration sensor. Adv Funct Mater. 2014;24:1401–1407.
[74] Niu S, Wang S, Liu Y, et al. A theoretical study of grating structured triboelectric nanogenerators. Energy Environ Sci. 2014;7:2339–2349.
[75] Zhu G, Lin Z-H, Jing Q, et al. Toward large-scale energy harvesting by a nanoparticle-enhanced triboelectric nanogenerator. Nano Lett. 2013;13:847–853.
[76] Jing Q, Kar-Narayan S. Nanostructured polymer-based piezoelectric and triboelectric materials and devices for energy harvesting applications. J Phys D Appl Phys. 2018;51:303001.
[77] Jeong CK, Baek KM, Niu S, et al. Topographically-designed triboelectric nanogenerator via block copolymer self-assembly. Nano Lett. 2014;14:7031–7038.
[78] Kim D, Jeon S-B, Kim JY, et al. High-performance nanopattern triboelectric generator by block copolymer lithography. Nano Energy. 2015;12:331–338.
[79] Wang HS, Jeong CK, Seo M-H, et al. Performance-enhanced triboelectric nanogenerator enabled by wafer-scale nanograte of multistep pattern downscaling. Nano Energy. 2017;35:415–423.
[80] Feng Y, Zheng Y, Ma S, et al. High output polypropylene nanowire array triboelectric nanogenerator through surface structural control and chemical modification. Nano Energy. 2016;19:48–57.
[81] Wang S, Xie Y, Niu S, et al. Maximum surface charge density for triboelectric nanogenerators achieved by ionized-air injection: methodology and theoretical understanding. Adv Mater. 2014;26:6720–6728.
[82] Wang S, Zi Y, Zhou YS, et al. Molecular surface functionalization to enhance the power output of triboelectric nanogenerators. J Mater Chem A. 2016;4:3728–3734.
[83] Lin Z-H, Xie Y, Yang Y, et al. Enhanced triboelectric nanogenerators and triboelectric nanosensor using chemically modified TiO_2 nanomaterials. ACS Nano. 2013;7:4554–4560.
[84] Lin W-C, Lee S-H, Karakachian M, et al. Tuning the surface potential of gold substrates arbitrarily with self-assembled monolayers with mixed functional groups. Phys Chem Chem Phys. 2009;11:6199.
[85] Zhou YS, Liu Y, Zhu G, et al. *In situ* quantitative study of nanoscale triboelectrification and patterning. Nano Lett. 2013;13:2771–2776.
[86] Byun K-E, Cho Y, Seol M, et al. Control of triboelectrification by engineering surface dipole and surface electronic state. ACS Appl Mater Interfaces. 2016;8:18519–18525.
[87] Sano C, Mitsuya H, Ono S, et al. Triboelectric energy harvesting with surface-charge-fixed polymer based on ionic liquid. Sci Technol Adv Mater. 2018;19:317–323.
[88] Yang W, Chen J, Zhu G, et al. Harvesting energy from the natural vibration of human walking. ACS Nano. 2013;7:11317–11324.
[89] Lee S, Lee Y, Kim D, et al. Triboelectric nanogenerator for harvesting pendulum oscillation energy. Nano Energy. 2013;2:1113–1120.
[90] Zhong J, Zhong Q, Fan F, et al. Finger typing driven triboelectric nanogenerator and its use for instantaneously lighting up LEDs. Nano Energy. 2013;2:491–497.
[91] Kim D, Tcho I-W, Jin IK, et al. Direct-laser-patterned friction layer for the output enhancement of a triboelectric nanogenerator. Nano Energy. 2017;35:379–386.

[92] Kim SJ, Lee HE, Choi H, et al. High-performance flexible thermoelectric power generator using laser multiscanning lift-off process. ACS Nano. 2016;10:10851–10857.
[93] Park WI, You BK, Mun BH, et al. Self-assembled incorporation of modulated block copolymer nanostructures in phase-change memory for switching power reduction. ACS Nano. 2013;7:2651–2658.
[94] Jin HM, Lee SH, Kim JY, et al. Laser writing block copolymer self-assembly on graphene light-absorbing layer. ACS Nano. 2016;10:3435–3442.
[95] Choi H-J, Lee JH, Jun J, et al. High-performance triboelectric nanogenerators with artificially well-tailored interlocked interfaces. Nano Energy. 2016;27:595–601.
[96] Pourrahimi AM, Olsson RT, Hedenqvist MS. The role of interfaces in polyethylene/metal-oxide nanocomposites for ultrahigh-voltage insulating materials. Adv Mater. 2018;30:1703624.
[97] Wei XY, Zhu G, Wang ZL. Surface-charge engineering for high-performance triboelectric nanogenerator based on identical electrification materials. Nano Energy. 2014;10:83–89.
[98] Wang Z, Cheng L, Zheng Y, et al. Enhancing the performance of triboelectric nanogenerator through prior-charge injection and its application on self-powered anticorrosion. Nano Energy. 2014;10:37–43.
[99] Choi YS, Jing Q, Datta A, et al. A triboelectric generator based on self-poled Nylon-11 nanowires fabricated by gas-flow assisted template wetting. Energy Environ Sci. 2017;10:2180–2189.
[100] Yun BK, Kim JW, Kim HS, et al. Base-treated polydimethylsiloxane surfaces as enhanced triboelectric nanogenerators. Nano Energy. 2015;15:523–529.
[101] Hoek I, Tho F, Arnold WM. Sodium hydroxide treatment of PDMS based microfluidic devices. Lab Chip. 2010;10:2283.
[102] Yao C, Yin X, Yu Y, et al. Chemically functionalized natural cellulose materials for effective triboelectric nanogenerator development. Adv Funct Mater. 2017;27:1700794.
[103] Shang W, Gu GQ, Yang F, et al. A sliding-mode triboelectric nanogenerator with chemical group grated structure by shadow mask reactive ion Etching. ACS Nano. 2017;11:8796–8803.
[104] Shin S-H, Bae YE, Moon HK, et al. Formation of triboelectric series via atomic-level surface functionalization for triboelectric energy harvesting. ACS Nano. 2017;11:6131–6138.
[105] Busolo T, Ura DP, Kim SK, et al. Surface potential tailoring of PMMA fibers by electrospinning for enhanced triboelectric performance. Nano Energy. 2019;57:500–506.
[106] Liu L, Tang W, Wang ZL. Inductively-coupled-plasma -induced electret enhancement for triboelectric nanogenerators. Nanotechnology. 2017;28:035405.
[107] Lai M, Du B, Guo H, et al. Enhancing the output charge density of TENG via building longitudinal paths of electrostatic charges in the contacting layers. ACS Appl Mater Interfaces. 2018;10:2158–2165.
[108] Huang T, Lu M, Yu H, et al. Enhanced power output of a triboelectric nanogenerator composed of electrospun nanofiber mats doped with graphene oxide. Sci Rep. 2015;5:13942.
[109] Wu C, Kim TW, Choi HY. Reduced graphene-oxide acting as electron-trapping sites in the friction layer for giant triboelectric enhancement. Nano Energy. 2017;32:542–550.
[110] Uddin ASMI, Yaqoob U, Chung G-S. Improving the working efficiency of a triboelectric nanogenerator by the semimetallic PEDOT:PSS hole transport layer and its application in self-powered active acetylene gas sensing. ACS Appl Mater Interfaces. 2016;8:30079–30089.
[111] Bai P, Zhu G, Zhou YS, et al. Dipole-moment-induced effect on contact electrification for triboelectric nanogenerators. Nano Res. 2014;7:990–997.
[112] Kang H, Kim H, Kim S, et al. Mechanically robust silver nanowires network for triboelectric nanogenerators. Adv Funct Mater. 2016;26:7717–7724.
[113] Kwon YH, Shin S-H, Kim Y-H, et al. Triboelectric contact surface charge modulation and piezoelectric charge inducement using polarized composite thin film for performance enhancement of triboelectric generators. Nano Energy. 2016;25:225–231.
[114] Lee KY, Kim SK, Lee J-H, et al. Controllable charge transfer by ferroelectric polarization mediated triboelectricity. Adv Funct Mater. 2016;26:3067–3073.
[115] Yang X, Daoud WA. Triboelectric and piezoelectric effects in a combined tribo-piezoelectric nanogenerator based on an interfacial ZnO nanostructure. Adv Funct Mater. 2016;26:8194–8201.
[116] Peng J, Kang SD, Snyder GJ. Optimization principles and the figure of merit for triboelectric generators. Sci Adv. 2017;3:eaap8576.
[117] Liu D, Hoang AT, Pourrahimi AM, et al. Influence of nanoparticle surface coating on electrical conductivity of LDPE/Al_2O_3 nanocomposites for HVDC cable insulations. IEEE Trans Dielectr Electr Insul. 2017;24:1396–1404.
[118] Chun J, Kim JW, Jung W, et al. Mesoporous pores impregnated with Au nanoparticles as effective dielectrics for enhancing triboelectric nanogenerator performance in harsh environments. Energy Environ Sci. 2015;8:3006–3012.
[119] Lee JW, Cho HJ, Chun J, et al. Robust nanogenerators based on graft copolymers via control of dielectrics for remarkable output power enhancement. Sci Adv. 2017;3:e1602902.
[120] Seung W, Yoon H-J, Kim TY, et al. Boosting power-generating performance of triboelectric nanogenerators via artificial control of ferroelectric polarization and dielectric properties. Adv Energy Mater. 2017;7:1600988.
[121] Kim J, Lee JH, Ryu H, et al. High-performance piezoelectric, pyroelectric, and triboelectric nanogenerators based on P(VDF-TrFE) with controlled crystallinity and dipole alignment. Adv Funct Mater. 2017;27:1700702.
[122] Šutka A, Mālnieks K, Linarts A, et al. Inversely polarised ferroelectric polymer contact electrodes for triboelectric-like generators from identical materials. Energy Environ Sci. 2018;11:1437–1443.
[123] Kim S, Gupta MK, Lee KY, et al. Transparent flexible graphene triboelectric nanogenerators. Adv Mater. 2014;26:3918–3925.
[124] Dong Y, Mallineni SSK, Maleski K, et al. Metallic MXenes: A new family of materials for flexible

triboelectric nanogenerators. Nano Energy. 2018;44:103–110.
[125] Wu C, Kim TW, Park JH, et al. enhanced triboelectric nanogenerators based on MoS_2 monolayer nanocomposites acting as electron-acceptor layers. ACS Nano. 2017;11:8356–8363.
[126] Seol M, Kim S, Cho Y, et al. Triboelectric series of 2D layered materials. Adv Mater. 2018;30:1801210.
[127] Li S, Wang S, Zi Y, et al. Largely improving the robustness and lifetime of triboelectric nanogenerators through automatic transition between contact and non-contact working states. ACS Nano. 2015;9:7479–7487.